Future projections of wind resource in a mountainous archipelago, Canary Islands

Albano González*, Juan C. Pérez, Juan P. Díaz, Francisco J. Expósito*

Grupo de Observación de la Tierra y la Atmósfera (GOTA), Universidad de La Laguna (ULL), Canary Islands, Spain

Abstract

Large-scale atmospheric patterns and near-surface winds are expected to be modified in the future due to climate change, altering the availability of wind resources on a regional scale. These possible changes are especially important in isolated power systems, as is the case for a great percentage of the islands. High-resolution climate regionalization is therefore necessary to assess the future projections of wind resource, mainly in the case of orographically complex territories, such as The Canary Islands. In this work, WRF was used to perform a dynamic regionalization in this Archipelago, using the pseudo-global warming technique to compute the initial and boundary conditions from a reanalysis dataset and from the monthly mean changes obtained from the simulations of fourteen global climate models included in the Coupled Model Intercomparison Project Phase 5 (CMIP5). Projections of mean wind, wind energy density and extractable wind power were obtained for two future decades (2045-2054 and 2090-2099) and for two different greenhouse gas scenarios (RCP4.5 and RCP8.5) and the results were compared with those for 1995-2004. Statistically significant changes in wind resource were found in some areas, mainly during summer. Most of these areas correspond to zones where at present wind farms are located.

Keywords: Wind power, Climate change, energy projections, Canary Islands

1. Introduction

The Canary Islands is a Spanish archipelago, being the most populated territory of all the outermost regions in the European Union. It is located

*Corresponding author
Email address: aglezf@ull.edu.es (Albano González)

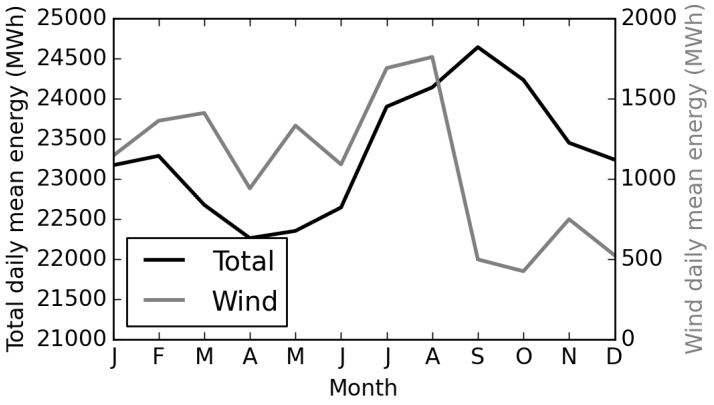

Figure 1: Total energy demand and wind energy production in the Canary Islands, expressed as daily mean values, for the last two years (2014 and 2015).

to the North-West of the African coast, centered approximately at 28^{o}N, 16^{o}W. This archipelago is made up of seven islands: Tenerife, Fuerteventura, Gran Canaria, Lanzarote, La Palma, La Gomera and El Hierro, and additional islets. The electricity system of Canary Islands is broken down into six electrically isolated subsystems, one per island except for Lanzarote and Fuerteventura, whose grids are joined by a submarine cable. The fact that the systems are isolated, which increases the difficulty of system optimization as a whole, to ensure the quality of the service, and the variability of the renewable energy production due to changing weather conditions, makes the development of the renewable energy market more difficult than in larger power systems. However, the Archipelago, due to its climate characteristics, has an abundant supply of renewable energy sources, mainly from the wind and sun. Renewable energies are particularly relevant in El Hierro, where a wind-hydro power station has been connected to five wind-powered generators, creating the first isolated territory in the world to meet all its energy needs using renewables [1]. For this reason, some plans for wind energy development in The Canary Islands have been implemented in the recent decades [2]. At present, the total installed power is approximately 3000 MW. From all this power, 1729 MW correspond to fuel/gas, 918 MW are generated by combined cycle power stations, 166 MW are provided by solar photovoltaic plants and 154 MW by wind farms [3]. The energy demand in The Canary Islands presents a clear annual cycle, with a higher power consumption during summer and at the beginning of autumn and with lower demand during spring. In Figure 1 the annual cycle for the last two years is plotted, based on the data provided by the transmission agent and operator of the Spanish electricity system [4]. The annual cycle of the wind energy production in the

Archipelago is also shown in the figure, where the higher production corresponds to summer, when the trade winds are stronger and more persistent.

Selecting a location for wind farm placement involves several factors, such as adequate land rights, official permits, environmental impact assessment, proximity and convenient access to existing power grids, investors and, of course, adequate wind to achieve the expected level of energy production. Since the wind power density is proportional to the cube of its speed [5], small changes in wind speed can make significant difference in the output of a wind farm. At any particular location, the wind direction and speed depends on several factors, such as synoptic atmospheric circulation, surface energy flows and local surface properties and topography. Due to these complex relationships, a detailed wind climatology is necessary to assess wind resources in a region. Formerly, these climatologies were mainly obtained from weather station data. However, due to the costs associated with the installation of a sufficient number of stations, needed to obtain a detailed map of wind resources, the results from numerical weather prediction (NWP) models are increasingly used [6].

Changes in synoptic wind patterns are expected in the future due to global climate change, which in turn will cause a modification of the winds at a regional scale, affecting the potential to generate power at a particular location. These possible changes in wind resources could influence the choice of preferential locations for wind farms, especially if long-term operation and investment is planned. Global climate models (GCMs) have been used as an effective tool to simulate many aspects of large-scale and global climate and to study the possible changes due to the global warming. Many of these studies are regularly summarised in the IPCC (Intergovernmental Panel on Climate Change) reports. Although GCMs incorporate the main characteristics of the general circulation patterns, their applicability to regional climate impact studies is limited because their typical spatial resolutions are in the order of hundreds of kilometers, which is too coarse to provide useful climate information for applications at regional-scale regimes. Furthermore, at those coarse resolutions, the topography is not well represented, which is an additional disadvantage to properly solve the physical processes in some regions, such as in those where the orography is complex. To overcome these inconveniences, regional climate models (RCMs) are required, allowing a better and more precise description of atmospheric events that are produced at smaller scales. In this way, statistical and dynamical downscaling methods have been developed in recent decades to improve the projections of local climate simulations provided by GCMs.

Several climate regionalization studies have investigated the potential future changes in wind for Europe [7, 8, 9] and other continents or countries

[10, 11, 12] using different regional climate models (RCM) and specifically for Spain [13], with a higher spatial resolution. They found a general decrease in wind speed, especially in the center of the Iberian Peninsula and on the Mediterranean coast. However, these studies did not include the Canary Islands, which are distant from the European continent and with such a complex topography that requires RCM simulations with high spatial resolution.

This work aims to estimate future changes in wind properties in the Canarian Archipelago, in the middle and at the end of this century. In this study the pseudo-global warming (PGW) method [14, 15, 16] has been used to perform a dynamical regionalization of wind climatology for The Canary Islands, and the Weather Research and Forecasting (WRF) model [17] was selected as the regional climate model (RCM).

The outline of this article is as follows. The configuration of WRF to obtain wind simulations for present and future periods is described in Section 2. In this section the observational data used to compare wind simulation assessment and the corresponding statistical indicators used to evaluate wind speed, wind energy density and extractable wind power are also exposed. In Section 3 the results for both, present period simulation assessment and future projections, are presented. Finally, the conclusions are summarised in the last section.

2. Methodology and data.

In this section the configuration of the WRF model and the input data of projected scenarios obtained through the PGW method from the reanalysis data and from the results of the CMIP5 global climate models are explained. The observational data used for the model assessment and the metrics chosen for this study are also exposed. Finally, the procedures used to estimate the wind energy density and the extractable wind power are outlined.

2.1. Model setup.

WRF, version 3.4.1 , was used to perform the downscaling simulations, using three domains in a double-nested configuration, with spatial resolutions of 45, 15, and 5 km (Fig. 2). All of these domains have been discretized with 32 vertical eta levels. The selection of the physical parameterizations, to represent the different sub-grid scale atmospheric processes, was done according to previous studies in the same area [18, 19]. Thus, radiation schemes were set to the Community Atmosphere Model, version 3 (CAM3), for computing both longwave and shortwave radiation fluxes [20]. In the coarser resolution domains, D1 and D2, where the fluxes cannot be explicitly resolved,

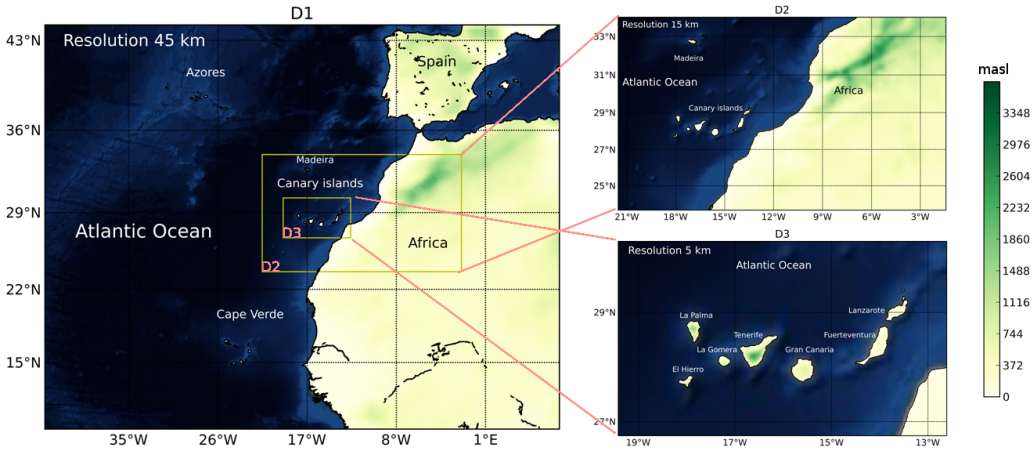

Figure 2: Domains used in the WRF simulations. The coarse domain (D1) has a horizontal resolution of 45 km, D2 of 15-km, and the innermost domain (D3) a resolution of 5 km, covering the Canary Islands region. Color shades indicate land surface height (m asl).

Kain-Fritsch cumulus parameterization [21] was used, and no cumulus parameterization was applied in the innermost domain, which has an horizontal resolution under 10 km. The planetary boundary layer was characterized using the Yonsei University scheme [22] and the land surface using the Noah model [23]. Finally, the WRF double-moment 6-class (WDM6) [24] was used as a cloud microphysics scheme.

In this work the PGW approximation was used for climate regionalization following the same configuration used in a previous study [26], in which future changes in temperature and precipitation were analysed. Thus, WRF initial and boundary conditions for a recent period (1995-2004) were directly taken from ERA-Interim reanalysis data [27]. This constitutes one of the main advantages of this method, because the errors in simulating observed climate caused by biases in the boundary conditions from global climate models are largely diminished [14]. For future periods, in our case 2045-2054 and 2090-2099, initial and boundary conditions for the WRF integrations are given by the sum of a climate perturbation signal to the same ERA-Interim data used for the present simulation. This signal was computed, for those variables of interest, from the results of 14 GCMs (Table 1) projections averaging their monthly mean values [26]. All the GCM projections belong to the Coupled Model Intercomparison Project Phase 5 (CMIP5). For each future period two different greenhouse gas concentration pathways, the CMIP5 RCP4.5 and RCP8.5 scenarios [28] were used. These scenarios represent middle and high emission assumptions, using emission pathways which lead to radiative forcings of 4.5 and 8.5 Wm^{-2} at the end of this century, that correspond

Table 1: CMIP5 models used in this work to obtain the ensemble of perturbation signal for the PGW method. More information about models and the main references for each of them can be found in [25].

Model	Institution(s)	Country
ACCESS1.3	Commonwealth Scientific and Industrial Research Organization (CSIRO) and Bureau of Meteorology (BOM)	Australia
BCC-CSM1.1	Beijing Climate Center, China Meteorological Administration	China
CanESM2	Canadian Center for Climate Modelling and Analysis	Canada
CCSM4	US National Centre for Atmospheric Research	United States
CSIRO-Mk3.6.0	Queensland Climate Change Centre of Excellence and Commonwealth Scientific and Industrial Research Organisation	Australia
EC-EARTH	Europe	Europe
GFDL-ESM2G	NOAA Geophysical Fluid Dynamics Laboratory	United States
HadGEM2-ES	UK Met Office Hadley Centre	United Kingdom
INM-CM4	Russian Institute for Numerical Mathematics	Russia
IPSL-CM5A-MR	Institut Pierre Simon Laplace	France
MIROC5	University of Tokyo, National Institute for Environmental Studies, and Japan Agency for Marine-Earth Science and Technology	Japan
MPI-ESM-MR	Max Planck Institute for Meteorology	Germany
MRI-ESM1	Meteorological Research Institute	Japan
NorESM1-M	Norwegian Climate Centre	Norway

to greenhouse gas concentrations of approximately 650 and 1370 ppm CO_2 equivalent, respectively [29]. For each experiment the model was integrated continuously for an eleven-year period, taking the first year as spin-up, which is not considered in any further analysis.

The PWG method allows us to use shorter simulation periods [30, 31], which is another of the advantages of this method for those regions that, due to their topography, require high resolution simulations and, therefore, high computational efforts. Despite the mentioned advantages of PGW, this approximation also has limitations, such as the inadequate simulation of possible changes in the variability from daily to inter-annual timescales, because it assumes unchanged variability in the future climate. It also assumes that the frequency and intensity of weather perturbations that enter the regional simulation domain remain unchanged, making this method inadequate for studying extreme wind events, which can affect wind turbine design due to their effect in fatigue loads.

2.2. Observational data.

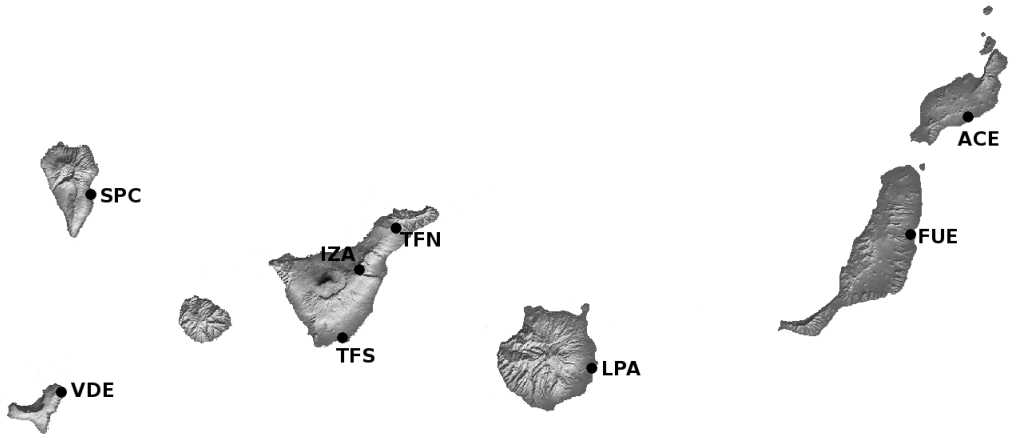

Figure 3: Location of the stations used for WRF wind results assessment

Wind speed and direction simulated by the WRF model in the present period (1995-2004) must be validated using observational data. In this case observational records obtained from the Spanish Meteorological Agency (Agencia Estatal de Meteorología - AEMET) were used. From all the available stations, those with more than 10% of missing values for the selected period were discarded, therefore leaving 8 stations remaining (Fig. 3). They correspond to the airport stations, except the IZA station that is located in the

Izaña Atmospheric Observatory at 2371 m asl. The hourly data recordings for these stations were averaged obtaining daily mean values.

Usually, observational data are clustered to facilitate the comparison with simulation results using homogeneous regions [13]. However, the number of available wind stations and the complex orography resulted in the clustering methods used in previous works [19] in the same Archipelago, for temperature and precipitation, failing to provide adequate results. Therefore, the comparisons were made for each individual observational site.

The WRF simulation ability to reproduce daily mean wind speed was assessed through the bias and root mean square error, taking into account, for each station, only those days for which observational data were available. The probability density functions (PDFs) were also computed with daily wind speed data series, to evaluate the simulation skills in reproducing the wind variability. To compare the PDFs from observational data and WRF simulation, the Perkins skill score [32] was selected. This measures the similarity between two PDFs, computing the common area of both distributions:

$$S_{score} = \sum_{i=1}^{n} minimum\Big(P_o(i), P_s(i)\Big) \tag{1}$$

where $P_o(i)$ and $P_s(i)$ are the frequency of the observed and simulated wind speed, respectively, in the i-th bin of the total n bins used to obtain the PDFs.

For the validation of the wind direction, the wind roses of observed and simulated winds were analysed, and the directional accuracy (DACC) parameter [33] was used. DACC is defined as the percentage of days for which the wind direction of observations and simulated values differ less than 20^o.

2.3. Energy density and extractable wind power estimation.

In addition to wind speed, the wind energy density (WED), that is the kinetic energy flux associated with the winds, is commonly used to assess the implications of possible future wind speed changes for the wind energy resource in any particular region [7, 8, 34]. It is defined as

$$WED = \frac{1}{2}\rho U^3 \tag{2}$$

where U is the wind speed and ρ the air density, taken equal to 1.225 kg m^{-3}. U must be computed at the turbine hub height, which for this study is considered to be at 80 m. To extrapolate U from 10 m, the height at which the surface wind is provided by WRF, to 80 m the power law is used, as suggested in [7]

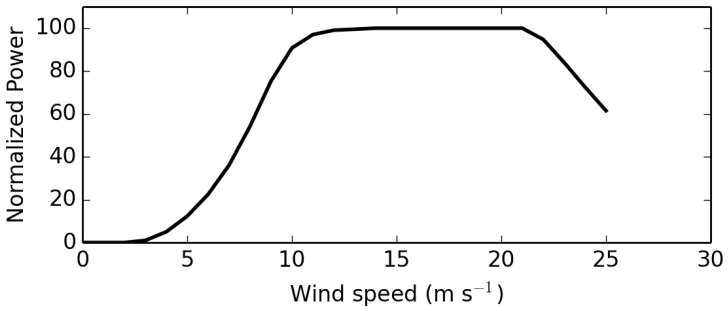

Figure 4: Power curve of a typical modern turbine (GAMESA-G97-2MW) normalized by the turbine nominal power.

$$U_{80} = U_{10} \left(\frac{80}{10} \right)^{\alpha} \tag{3}$$

where α is set to 0.2 for onshore areas and of 0.14 for offshore sites, based on the recommendations of the International Electrotechnical Commission (IEC).

Although, WED is a measure of the potential power that can be produced by wind turbines, it does not account for the fact that turbines generate power only for a limited range of wind speeds. The lower limit, the cut-in speed, is typically between 3 and 4 m s^{-1} and corresponds to the speed at which the turbine first starts to rotate and generate power. The upper limit, the cut-out speed, is fixed to avoid the risk of damage to the rotor and is usually around 25 m s^{-1}. For this reason, in order to get an assessment of the possible effects of climate change in power production due to changes not only in mean wind speed but also in wind speed distribution, the output of a typical turbine was also evaluated, as proposed in previous works [7, 8]. In this study, the GAMESA G97-2MW turbine was selected, which has a cut-in speed of 3 m s^{-1}, a rated-speed of approximately 11 m s^{-1}, a cut-out speed of 25 m s^{-1} and a rated output power of 2MW. To normalize the power results, making them independent of the nominal power of the turbine, the power curve was normalized (Fig. 4). Using this curve and the simulated wind, extrapolated to the hub height, 80 m, the power output of this normalized wind turbine was computed, and referred to as Extractable Wind Power (EWP). Both, WED and EWP were calculated from 2-hour time series for each WRF simulation.

2.4. Assessment of changes in wind speed, WED and EWP.

Annual and seasonal changes in mean wind speed, WED and EWP for the two selected future decades (2045-2054 and 2090-2099) and the two emission

scenarios (RCP4.5 and RCP8.5) with respect to the present decade (1995-2004) have been assessed. To establish the statistical significance of the simulated changes, a non parametric technique has been used, in order to avoid the restrictions of traditional parametric methods, which assume that data follows a particular distribution and the observed or simulated data are composed of independent samples from their parent populations. Specifically, a moving block bootstrap algorithm, which takes into account the effects of data autocorrelation, has been implemented [35]. From the possible time series models, the autoregressive-moving average process, of order 1 in both contributions, that is ARMA(1,1), has been selected based on previous evaluations of this method for other variables in The Canary Islands [26] and the study of the variables used in this work. For each grid point of the innermost domain, the corresponding ARMA(1,1) model was computed using daily time series and, based on its characteristics, the block length for the bootstrap test and the adjusted data variance for the test statistic were computed [35].

3. Results

In this section, the WRF simulation results for the present period are evaluated and the projected changes in wind resources for the two future periods and two greenhouse gases emission scenarios are exposed.

3.1. Daily-mean wind assessment.

The WRF present simulation results have been compared with observational data from all available stations, taking the closest grid point of the innermost domain. Due to the complex orography of Canary Islands, with altitude variations up to 3000 m in less than 20 km horizontally, and the spatial resolution of the innermost domain, significant differences between the height of weather stations and the height of the closest cell in the WRF simulation can arise. Both datasets have been compared as provided by observations and simulations, that is, at 10 m height and not interpolated to 80 m. The summary of these results are presented in Table 2, where the location and altitude of the observational stations and their corresponding closest grid points are also shown. The biases for some stations are very low and for most locations are lower than 1 m s^{-1}, corresponding to relative biases lower than 20%, except for the IZA station located on a ridge of an orographically complex area. The RMSE is generally under 3 m s^{-1}. The Perkins skill score, that measures the similarity between the PDFs of observed and simulated wind speeds, is higher than 80%, excluding the IZA station. In top row of Figure 5 the PDFs of two representative locations are plotted. In both cases,

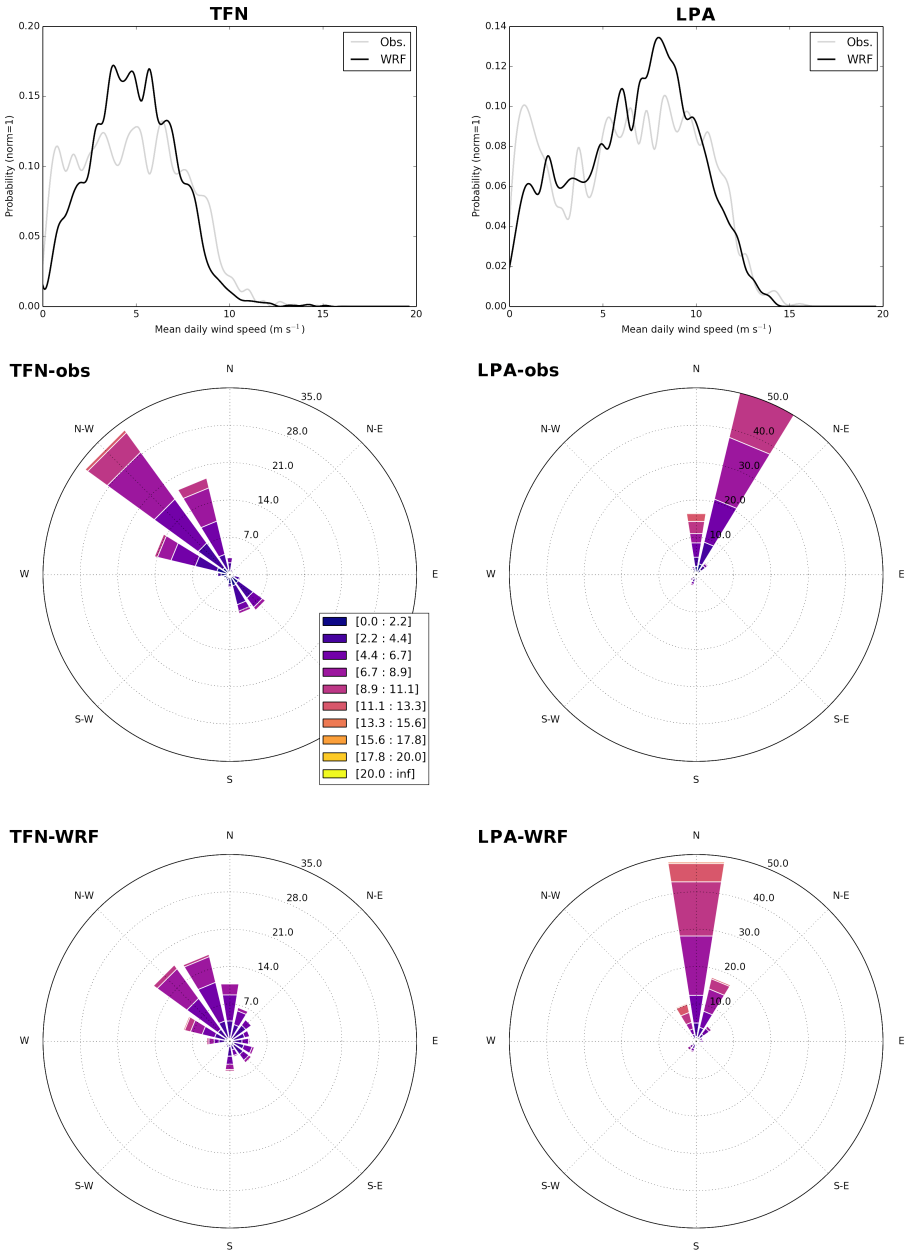

Figure 5: Top: probability distribution functions of daily surface wind speed derived from WRF simulations and observational data for 1995-2004 for two characteristic locations: TFN (left) and LPA (right). Corresponding wind roses derived from observational data (middle) and WRF simulations (bottom).

the WRF simulation provides very similar PDFs but overestimates slow wind speeds. The percentage of daily observations whose difference with the WRF

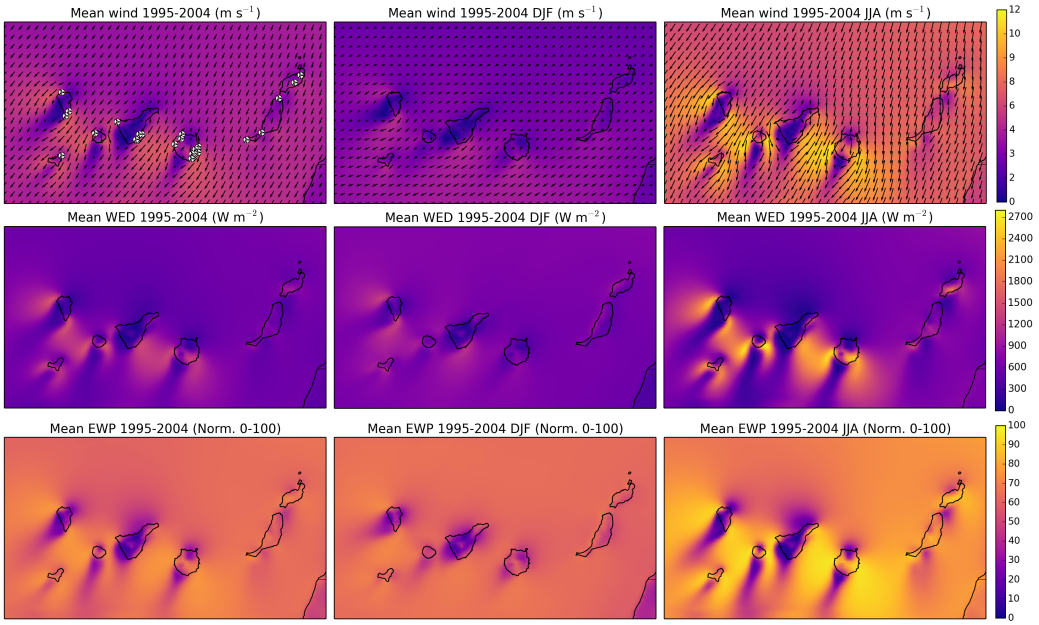

Figure 6: Top: annual and seasonal, for winter (December-January-February, DJF) and summer (June-July-August. JJA), mean wind speed (m s^{-1}) and direction for the present decade (1995-2004). Mid: annual and seasonal mean wind energy density (W m^{-2}). Bottom: annual and seasonal mean normalized extractable wind power, assuming the power curve of GAMESA-G97-2MW wind turbine.

simulated wind direction is lower than 20 degrees (DACC) is higher than 70% for most locations. This fact can be also appreciated in Figure 5, where the wind roses are represented for the same locations. The DACC values and this qualitative comparison between observed and modelled wind roses show that WRF simulation is able to reproduce the dominant wind direction.

3.2. Present wind resource and future projections.

To understand the importance of future changes, the knowledge of present wind climatology in The Canary Islands is necessary. For this reason, the annual mean wind speed and direction have been computed from present period WRF simulation (Fig. 6, top row). The present wind farm sites are also indicated in this figure. The highest mean wind speed areas generally correspond to the channels between higher islands. The preferred locations to install wind farms are the coasts of these zones. This geographic distribution of wind speed, is mainly driven by the persistent trade winds that affect the Archipelago and the main contribution to this pattern occurs during summer, when trade winds are strongest and more frequent, as previously commented, and it corresponds to the largest wind energy production season (Fig. 1).

Table 2: Weather stations acronyms, WMO (World Meteorological Organization) station identifiers (ID), heights (m asl), latitudes and longitudes (degrees), observed daily mean wind speed (m s^{-1}), latitude, longitude and height of the closest grid point in the innermost WRF domain (m asl), and the selected statistical parameters to evaluate WRF simulation results: bias (m s^{-1}), root mean square error (m s^{-1}), the Perkins skill score and the wind direction accuracy index (%).

Station	WMO	Observations				WRF simulations						
	ID	Lat. (deg.)	Lon. (deg.)	Height (m asl)	Mean (m s^{-1})	Lat. (deg.)	Lon. (deg.)	Height (m asl)	Bias (m s^{-1})	RMSE (m s^{-1})	Skill score	DAAC (%)
VDE	60001	27.82^{o}N	17.89^{o}W	32	5.45	27.82^{o}N	17.88^{o}W	146	0.72	2.99	0.88	73.3
LPA	60030	27.92^{o}N	15.39^{o}W	24	6.58	27.92^{o}N	15.38^{o}W	58	0.27	2.63	0.88	84.8
TFS	60025	28.05^{o}N	16.56^{o}W	64	4.84	28.07^{o}N	16.57^{o}W	63	1.01	2.69	0.83	80.3
IZA	60010	28.31^{o}N	16.50^{o}W	2371	6.22	27.32^{o}N	17.48^{o}W	1465	-3.63	5.47	0.50	66.7
FUE	60035	28.44^{o}N	13.86^{o}W	25	5.05	28.43^{o}N	13.87^{o}W	123	-0.01	2.78	0.91	70.6
TFN	60015	28.48^{o}N	16.33^{o}W	632	4.98	28.48^{o}N	16.33^{o}W	619	0.07	2.14	0.84	71.9
SPC	60005	28.63^{o}N	17.76^{o}W	32	3.97	28.63^{o}N	17.77^{o}W	522	0.02	1.63	0.89	66.5
ACE	60040	28.85^{o}N	13.60^{o}W	14	5.34	28.97^{o}N	13.58^{o}W	213	1.04	2.02	0.85	82.8

This behaviour can be deduced from Figure 6, top row, where the seasonal mean wind speed and direction are represented for winter and summer. In Figure 6, middle row, the annual and seasonal mean WED, for summer and winter, are also presented, clearly showing those areas where the wind energy density is very important. This magnitude is widely used for wind assessment studies, but, as previously explained, not all this potential can be used by wind turbines. So, the normalized EWP has been also displayed in that figure. Concerning the EWP (Fig. 6, bottom row), the preferred sites for the installation of wind farms can be detected, showing larger areas than those indicated by WED. This extends the possible location of wind turbines not only to certain zones of the coasts of the higher islands but also to some areas of Lanzarote and Fuerteventura, which have a lower orography. In all these areas, the normalized EWP is around 95 normalized units during summer, indicating that almost 100% of the maximum extractable power can be exploited.

Changes in wind speed, WED and EWP between future and present decades have been computed, for both annual and seasonal means. Statistically significant changes, at a 0.05 significance level, in wind speeds were only obtained in small areas of Lanzarote and Fuerteventura when annual results were considered. In this case, a slight increase, and only for the decade 2090-2099 and for the highest emission scenario, RCP8.5, can be observed. In the seasonal analysis, the majority of statistically significant changes in wind speed correspond to the summer, as shown in Figure 7. As expected, largest and most significant changes correspond to the RCP8.5 scenario. Changes in wind direction are not shown because they are very small and difficult to observe, but in summer the prevailing North-East wind backs slightly, with a larger component from the North. WED maps provided very similar results and they are not shown.

The EWP allows us to discern those areas where the projected wind speed changes could have a greater influence on the wind power production. Thus, in Figure 8 those regions where the changes in EWP for the summer season are statistically significant can be observed. The most important decreases in extractable wind power, up to 15-20% in the late century for the RPC8.5 scenario, are expected to be in the central part of La Palma, North coast of La Gomera and El Hierro, North and South-East coast of Tenerife, North and South coast of Gran Canaria, and North-West coast of Lanzarote and Fuerteventura. A significant increase of EWP, around 15%, can be observed in the East coast of La Palma, Tenerife, Gran Canaria, and Fuerteventura. In this last island the EWP also increases in the Southern part. Taking into account the locations of present wind farms (Figure 6), the projections show a decrease of extracted energy in La Palma, El Hierro, La Gomera

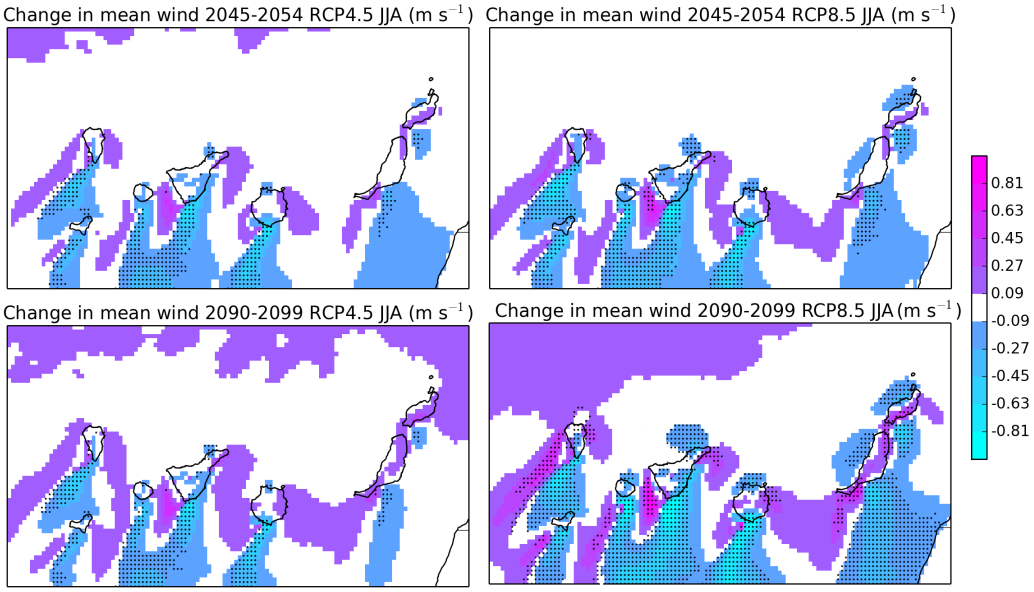

Figure 7: Mean wind speed differences (m s^{-1}) between future simulations and present for two periods: at the middle of the century (top) and at the end (bottom). Two greenhouse emission scenarios have been used: RCP4.5 (left) and RCP8.5 (right). Black dots indicate those areas where the changes are statistically significant.

and Tenerife. For Gran Canaria the most affected locations are those in the Northern and Southern part of the island. In Fuerteventura all the locations would be favoured by an increase of wind speed. Finally, present wind farms in Lanzarote would not be significantly affected.

4. Conclusions

The climate regionalization of natural resources, using high resolution numerical weather prediction models, such as WRF, provides useful results for orographically complex areas, which policymakers and investors should consider in future decisions about the preferential locations of wind farms and about the strategic planning for the energy networks. These results are specially important in islands with isolated power grids, as is the case of The Canary Islands. In this work the pseudo-global warming approach has been selected to obtain the regional projections of changes in wind resources in this Archipelago, reducing the computational cost of the high resolution simulations required in areas of complex topography and avoiding the problem of the global climate models biases in the present period. Although this technique is not adequate to evaluate the possible changes in extreme events, due to the assumption that the daily, seasonal or annual variability remains the

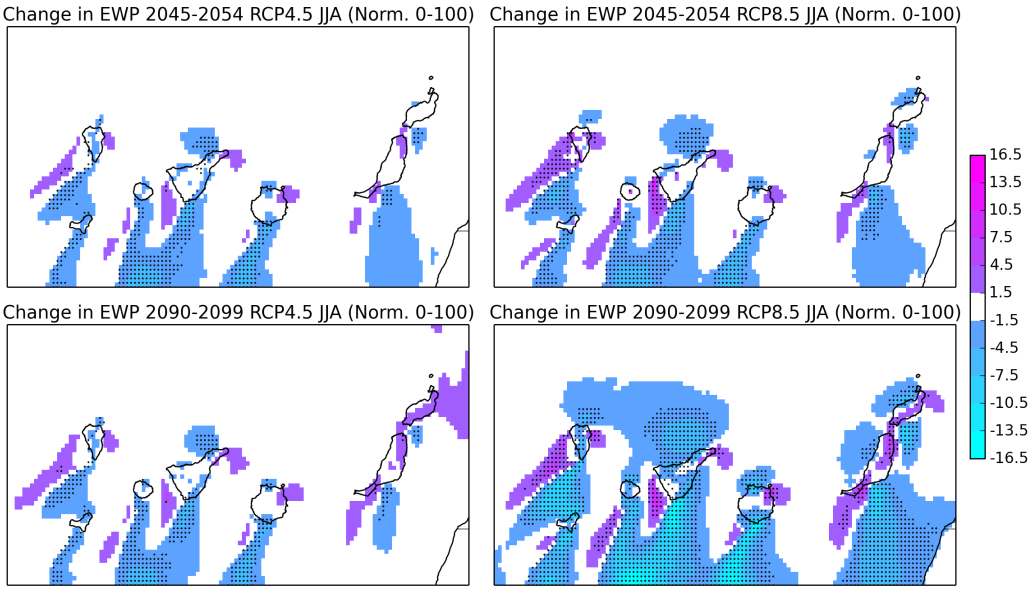

Figure 8: Same as Figure 7 but for EWP. Units are in normalized power, between 0 and 100.

same as in present period for the simulation of future decades, the changes in mean values of wind speed and direction, the wind energy density or the extractable wind power, can be assessed.

The present decade (1995-2004) simulation is able to reproduce the surface mean wind speed and its distribution when compared to observations located in the different islands and at several heights. The exception is an observational site (IZA) located at 2371 m asl, which is misrepresented in the model, with differences in the terrain height up to 900 m. To take into account these kind of cases, an increase in horizontal resolution and a better accuracy of the digital elevation model is desirable. However, these areas have not been considered as possible locations for wind farms, which in the case of The Canary Islands are mainly situated close to the coast. Furthermore, many of these high altitude areas have been declared national parks, where these infrastructures are forbidden.

Projected mean annual changes in surface wind speed for two future decades (2045-2054 and 2090-2099) with respect to the present decade are small and not statistically significant. However, considerable modifications can be observed at seasonal scale, mainly for summer. During winter a general increase of wind speed was noted for most of the studied region, but those changes are only significant in few simulation grid points. During summer, that corresponds to the season of maximum wind energy production in

the Archipelago, and significant changes can be appreciated in several areas of the different islands. When the EWP is considered, the areas affected by climate change are clearly discernible, and many of them correspond to locations where, at present, wind farms are installed. For the highest elevation islands, that is, the five western ones, a general EWP reduction, up to 15-20% at the end of this century, is predicted for their central part and their northern and Southern coasts, while an EWP increase, around 10-15%, in their North-East coasts is also observed. For the flattest islands, Lanzarote and Fuerteventura, a general increase is expected in the Northern and Southern areas, and a reduction in the North-West coast.

The possible modifications in wind resources due to climate change, as those exposed in this study, and not only wind climatologies based on past observational data and model simulations, should be taken into account in the planning of new wind farms or the development of the current ones. Despite the relevance of the results shown in this work using the PGW methodology, a comprehensive regionalization of future climate scenarios, that requires multiple simulations, using a different GCM to compute the boundary conditions for each of them, should be implemented in the future. Furthermore, such studies will permit the analysis of the extremes, which are important for estimating possible damages to wind turbines and to analyze fatigue loads.

Acknowledgement

The authors acknowledge the MEC (Ministry of Education and Science, Spain) for the Projects CGL2010-21366-C04-01 and CGL2015-67508-R. Authors also thank the CLIMATIQUE Project co-financed by the Programa de Cooperación Transfronteriza España-Fronteras Exteriores 2008-2013 (POCTEFEX), the European Union funds and FEDER program. The weather station's data were obtained from the Meteorological State Agency of Spain (AEMET) and the ERA-Interim data were provided by the European Centre for Medium-Range Weather Forecasts (ECMWF). We also acknowledge the World Climate Research Programme's Working Group on Coupled Modelling, which is responsible for CMIP, and we thank the climate modeling institutions (listed in Table 1) for producing and making their model output available. For CMIP the U.S. Department of Energy's Program for Climate Model Diagnosis and Intercomparison provides coordinating support and led development of software infrastructure in partnership with the Global Organization for Earth System Science Portals. The WRF simulations performed in this study were managed by WRF4G.

References

[1] The Wind-Hydro-Pumped Station of El Hierro, http://www.goronadelviento.es, accessed: 2015-11-30.

[2] R. Calero, J. Carta, Action plan for wind energy development in the Canary Islands, Energy Policy 32 (10) (2004) 1185 – 1197. doi:http://dx.doi.org/10.1016/S0301-4215(03)00082-X.

[3] REE, The spanish electricity system 2014, Tech. rep., Red Eléctrica de España, Madrid, Spain (June 2015).
URL http://www.ree.es/en/publications/statistical-data-of-spanish-electrical-system/annual-report/spanish-electricity-system-2014

[4] Red eléctrica de españa, http://www.ree.es, accessed: 2015-11-30.

[5] J. F. Manwell, J. G. McGowan, A. L. Rogers, Wind energy explained theory, design and application, Wiley, 2009.

[6] S. Al-Yahyai, Y. Charabi, A. Gastli, Review of the use of numerical weather prediction (nwp) models for wind energy assessment, Renewable and Sustainable Energy Reviews 14 (9) (2010) 3192 – 3198. doi:http://dx.doi.org/10.1016/j.rser.2010.07.001.

[7] H. Hueging, R. Haas, K. Born, D. Jacob, J. G. Pinto, Regional Changes in Wind Energy Potential over Europe Using Regional Climate Model Ensemble Projections, J. Appl. Meteor. Climatol. 52 (4) (2013) 903917. doi:10.1175/jamc-d-12-086.1.

[8] I. Tobin, R. Vautard, I. Balog, F.-M. Bron, S. Jerez, P. M. Ruti, F. Thais, M. Vrac, P. Yiou, Assessing climate change impacts on european wind energy from ensembles high-resolution climate projections, Climatic Change 128 (1-2) (2014) 99112. doi:10.1007/s10584-014-1291-0.

[9] I. Barstad, A. Sorteberg, M. dos Santos Mesquita, Present and future offshore wind power potential in northern Europe based on downscaled global climate runs with adjusted SST and sea ice cover, Renewable Energy 44 (2012) 398 – 405. doi:http://dx.doi.org/10.1016/j.renene.2012.02.008.

[10] T.-J. Chang, C.-L. Chen, Y.-L. Tu, H.-T. Yeh, Y.-T. Wu, Evaluation of the climate change impact on wind resources in taiwan strait, Energy Conversion and Management 95 (2015) 435 – 445. doi:http://dx.doi.org/10.1016/j.enconman.2015.02.033.

[11] D. L. Johnson, R. J. Erhardt, Projected impacts of climate change on wind energy density in the united states, Renewable Energy 85 (2016) 66 – 73. doi:http://dx.doi.org/10.1016/j.renene.2015.06.005.

[12] D. J. Sailor, M. Smith, M. Hart, Climate change implications for wind power resources in the northwest united states, Renewable Energy 33 (11) (2008) 2393 – 2406. doi:http://dx.doi.org/10.1016/j.renene.2008.01.007.

[13] G. Gómez, W. D. Cabos, G. Liguori, D. Sein, S. Lozano-Galeana, L. Fita, J. Fernández, M. E. Magariño, P. Jiménez-Guerrero, J. P. Montávez, et al., Characterization of the wind speed variability and future change in the Iberian Peninsula and the Balearic Islands, Wind Energ.doi:10.1002/we.1893.

[14] F. Kimura, A. Kitoh, Downscaling by pseudo global warming method, The Final Report of ICCAP 4346.

[15] T. Sato, F. Kimura, A. Kitoh, Projection of global warming onto regional precipitation over Mongolia using a regional climate model, J. Hydrol. 333 (1) (2007) 144–154. doi:10.1016/j.jhydrol.2006.07.023.

[16] H. Kawase, T. Yoshikane, M. Hara, F. Kimura, T. Yasunari, B. Ailikun, H. Ueda, T. Inoue, Intermodel variability of future changes in the Baiu rainband estimated by the pseudo global warming downscaling method, J. Geophys. Res. 114 (D24). doi:10.1029/2009JD011803.

[17] W. C. Skamarock, J. B. Klemp, J. Dudhia, D. O. Gill, M. Barker, K. G. Duda, X. Y. Huang, W. Wang, J. G. Powers, A description of the Advanced Research WRF Version 3, Tech. rep., National Center for Atmospheric Research (2008).

[18] A. González, F. J. Expósito, J. C. Pérez, J. P. Díaz, D. Taima, Verification of precipitable water vapour in high-resolution WRF simulations over a mountainous archipelago, Quarterly Journal of the Royal Meteorological Society 139 (677) (2013) 2119–2133. doi:10.1002/qj.2092.

[19] J. Pérez, J. Díaz, A. González, J. Expósito, F. Rivera-López, D. Taima, Evaluation of WRF parameterizations for dynamical downscaling in Canary Islands, J. Climate (27) (2014) 5611–5631. doi:10.1175/JCLI-D-13-00458.1.

[20] W. D. Collins, P. J. Rasch, B. A. Boville, J. J. Hack, J. R. McCaa, D. L. Williamson, J. T. Kiehl, B. Briegleb, C. Bitz, S. Lin, et al., Description of the NCAR Community Atmosphere Model (CAM 3.0) (2004).

[21] J. S. Kain, J. M. Fritsch, A one-dimensional entraining/detraining plume model and its application in convective parameterization, J. Atmos. Sci. 47 (23) (1990) 2784–2802. doi:0.1175/1520-0469(1990)047<2784:AODEPM>2.0.CO;2.

[22] S.-Y. Hong, Y. Noh, J. Dudhia, A new vertical diffusion package with an explicit treatment of entrainment processes, Mon. Weather Rev. 134 (9) (2006) 2318–2341. doi:10.1175/MWR3199.1.

[23] F. Chen, J. Dudhia, Coupling an advanced land surface-hydrology model with the Penn State-NCAR MM5 modeling system. Part I: Model implementation and sensitivity, Mon. Weather Rev. 129 (4) (2001) 569–585. doi:10.1175/1520-0493(2001)129<0569:CAALSH>2.0.CO;2.

[24] K.-S. S. Lim, S.-Y. Hong, Development of an effective double-moment cloud microphysics scheme with prognostic cloud condensation nuclei (ccn) for weather and climate models, Mon. Weather Rev. 138 (5) (2010) 1587–1612. doi:10.1175/2009MWR2968.1.

[25] Intergovernmental Panel on Climate Change (Ed.), Climate Change 2013 - The Physical Science Basis, Cambridge University Press, Cambridge, 2013. doi:10.1017/cbo9781107415324.

[26] F. J. Expósito, A. González, J. C. Pérez, J. P. Díaz, D. Taima, High-resolution future projections of temperature and precipitation in the canary islands, Journal of Climate 28 (19) (2015) 7846–7856. doi:10.1175/JCLI-D-15-0030.1.

[27] D. Dee, S. Uppala, A. Simmons, P. Berrisford, P. Poli, S. Kobayashi, U. Andrae, M. Balmaseda, G. Balsamo, P. Bauer, et al., The ERA-Interim reanalysis: Configuration and performance of the data assimilation system, Q. J. Roy. Meteor. Soc. 137 (656) (2011) 553–597. doi:10.1002/qj.828.

[28] K. E. Taylor, R. J. Stouffer, G. A. Meehl, An overview of CMIP5 and the experiment design, B. Am. Meteorol. Soc. 93 (4) (2012) 485–498. doi:10.1175/BAMS-D-11-00094.1.

[29] D. P. Van Vuuren, J. Edmonds, M. Kainuma, K. Riahi, A. Thomson, K. Hibbard, G. C. Hurtt, T. Kram, V. Krey, J.-F. Lamarque, et al., The

representative concentration pathways: an overview, Climatic Change 109 (2011) 5–31. doi:10.1007/s10584-011-0148-z.

[30] H. Kawase, T. Yoshikane, M. Hara, B. Ailikun, F. Kimura, T. Yasunari, Downscaling of the climatic change in the Mei-yu rainband in East Asia by a pseudo climate simulation method, SOLA 4 (2008) 73–76. doi:10.2151/sola.2008-019.

[31] A. Lauer, C. Zhang, O. Elison-Timm, Y. Wang, K. Hamilton, Downscaling of climate change in the Hawaii region using CMIP5 results: On the choice of the forcing fields, J. Climate 26 (24) (2013) 10006–10030. doi:10.1175/JCLI-D-13-00126.1.

[32] S. E. Perkins, A. J. Pitman, N. J. Holbrook, J. McAneney, Evaluation of the AR4 climate models' simulated daily maximum temperature, minimum temperature, and precipitation over Australia using probability density functions, Journal of Climate 20 (17) (2007) 4356–4376. doi:10.1175/JCLI4253.1.

[33] F. J. Santos-Alamillos, D. Pozo-Vázquez, J. A. Ruiz-Arias, V. Lara-Fanego, J. Tovar-Pescador, Analysis of WRF model wind estimate sensitivity to physics parameterization choice and terrain representation in Andalusia (Southern Spain), J. Appl. Meteor. Climatol. Journal of Applied Meteorology and Climatology 52 (7) (2013) 15921609. doi:10.1175/jamc-d-12-0204.1.

[34] M. Gonçalves-Ageitos, A. Barrera-Escoda, J. M. Baldasano, J. Cunillera, Modelling wind resources in climate change scenarios in complex terrains, Renewable Energy 76 (2015) 670678. doi:10.1016/j.renene.2014.11.066.

[35] D. Wilks, Resampling hypothesis tests for autocorrelated fields, Journal of Climate 10 (1) (1997) 65–82.